SCIENCE CHINA
Information Sciences

• RESEARCH PAPER •
Special Focus on Internet of Minds

April 2020, Vol. 63 140312:1–140312:14
https://doi.org/10.1007/s11432-019-2763-5

Leader-following flocking for unmanned aerial vehicle swarm with distributed topology control

Chao LIU, Meng WANG, Qian ZENG & Wei HUANGFU*

Beijing Advanced Innovation Center for Materials Genome Engineering, School of Computer and Communication Engineering, University of Science and Technology Beijing, Beijing 100083, *China*

Received 26 September 2019/Revised 13 December 2019/Accepted 10 January 2020/Published online 9 March 2020

Abstract To address the flocking issues of an unmanned aerial vehicle (UAV) swarm operating at a leader-follower mode, distributed control protocols comprising both kinetic controller and topology control algorithm must be implemented. For flocking the UAV swarm, a distributed control-input method is required for both maintaining a relatively steady state between neighboring vehicles (including velocity matching and distance maintenance) and avoiding vehicle-to-vehicle collision. Furthermore, the stability of control protocols should be analyzed using the potential energy function. In particular, a distributed β-angle test (BAT) rule in the proposed topology-control issue may allow each UAV to determine its neighboring set by exploiting the locally sensed information, thereby significantly reducing the communication overhead of the entire swarm. In addition, node-degree bound is derived to demonstrate the feasibility of the proposed algorithm, in which the optimal value in terms of convergence is analyzed. The flocking of the flying ad-hoc network (FANET) can be achieved in a self-organizing way without the use of an external control center via the distributed control protocols. Ultimately, the proposed analysis is verified by numerical results.

Keywords flying ad hoc networks, flocking, leader-follower, topology control, neighbor selection

Citation Liu C, Wang M, Zeng Q, et al. Leader-following flocking for unmanned aerial vehicle swarm with distributed topology control. Sci China Inf Sci, 2020, 63(4): 140312, https://doi.org/10.1007/s11432-019-2763-5

1 Introduction

Owing to their flexible moving capabilities in the air, unmanned aerial vehicles (UAVs) or drones show a great potential of application in areas such as atmospheric research, emergency rescue, and cargo freight [1]. Different UAVs have various sizes and power consumption accordingly, depending on the diverse needs of their application scenarios [2]. Large-sized UAVs, in particular, are typically equipped with more sensors, high-capacity batteries, and more powerful engines, enabling them to execute complex tasks. If a failure occurs on a UAV, however, it will be difficult for it to resume its task. A UAV swarm comprising many lightweight UAVs is more robust than a single UAV scenario. Because these UAV swarms are redundant in quantity, they can tolerate some UAV failures during the mission.

However, in large-scale UAV swarms, the control strategy has become increasingly complicated, especially for centralized control schemes, in which the non-linearly increasing control overhead will seriously restrict the scalability and communication efficiency of the unmanned swarm. Furthermore, the control efficiency may be restricted by various issues, including the limited communication range of each UAV, the inter-UAV-interference and the propagation delay between individuals [3]. Therefore, we must resort to the distributed control mechanisms to improve the UAV swarm's control efficiency while achieving

* Corresponding author (email: huangfuwei@ustb.edu.cn)

© Science China Press and Springer-Verlag GmbH Germany, part of Springer Nature 2020

nearly the same goals as in centralized control [4]. The collective behavior of natural species, such as the group behavior of birds and fish swarms, can be regarded as a kind of spontaneously organized activity, which can provide useful inspirations to solve the above challenges [5–8]. Compared with the traditional centralized control-based network architecture, in a self-organizing network (SON) architecture, because each node can rely on local interactions with its neighbors to perform its communication tasks, the network's control signaling overhead can be greatly reduced by implementing the self-organizing mechanism. The swarm can be controlled by selecting one or more members as leaders to accomplish a number of specified tasks without requiring all members in the swam to maintain connections to the control center [9]. Obviously, the self-organizing control mechanism is very suitable for the drone group. By running the self-organizing control mechanism, it can exert excellent network control efficiency [10].

Notwithstanding, the UAV swarm's self-organizing mechanism still faces several challenges before its practical implementation, including the design of proper distributed neighbor selection rules and kinetic-input-and-topology-control mechanism for maintaining flocking, and the velocity consensus and collision avoidance among individuals [11]. To address these challenges, academia and industry have conducted extensive exploration.

• In a flying ad-hoc network (FANET) under the SON control rules, each individual UAV can obtain the motion state information of its neighbors located inside its communication range. Because each individual can act as a motion reference for its neighbors, it is essential for a swarm to converge by maintaining communication links among neighboring individuals in a real-time manner [12]. Furthermore, because each UAV is resource constrained with a limited communication efficiency, it is unnecessary for an individual UAV to establish a communication link with all of its neighboring nodes. In contrast, it is efficient for each UAV to establish a communication link with a part of its neighbors that have high channel qualities [13].

• Typical distributed topology control rules mainly comprise two rules, i.e., the link based and zone based rules. Explicilty, in link based rules such as the full-connectivity algorithm [14], the connection between any pair of neighbors can be created. On the other hand, in zone-based rules such as relative neighborhood graph (RNG), Yao graph (YG) and Gabriel graph (GG), a specific area must be identified in advance to act as the exclusion zone for potential interfering nodes [15]. However, full-connectivity algorithm may lead to redundancy connections to neighbors, especially in scenarios that the neighbor set is large. To address this issue, the optimal number of neighbors to form a robust flock with the least sensing cost is investigated [16], showing that it would be wonderful to ensure the algorithm's robustness and efficiency by considering only six to seven neighbors. Evidently, choosing N-nearest neighbors with a proper N value is likely to be preferred [17].

• In practice, the N-nearest rule exhibits drawbacks such as having asymmetric property and resulting in multiple subgroups [18]. Except for the above typical rules, Tian et al. [19] investigated the swarm of agents with a limited angle of view for tracking neighbors in the front-end by simulating the eyes of natural animals (which are asymmetric). Furthermore, in [20], an acute angle test (AAT) algorithm was proposed for solving the deployment problem of a large amount of robotic sensors, which is equivalent to determining the exclusion zone using Gabriel graph. In addition, Ning et al. [21] utilized the AAT rule to implement the neighbor-interaction rule of robots in two-dimensional spaces. However, the exclusion zone in [21] was merely determined by the distance between the transmitter and the receiver. Numerical results showed that in terms of convergence, this rule is not optimal. In addition, the node degree is not upper-bounded in the AAT-based topology control rule, making the protocol be less feasible in the application in a FANET [22].

• In kinetic-control problems, the primary goal of the controlling algorithm design is to develop a proper control function to adjust the motion status of UAVs as dynamic as needed. In general, the control function comprises two parts: (1) to maintain a relative distance between two neighbors; and (2) to achieve a velocity consensus among individuals. In particular, the distance-control functionality acts as a virtual force that provides an attractive or repulsive acceleration to the objects like a spring force. However, the function's curve is not necessarily linear. Furthermore, the part of velocity consensus, which can be utilized to guarantee the final velocity vector of each agent, is identical to its neighbors. In

addition, the convergence of the UAV swarm should be guaranteed by relying on the Lyapunov theory [23].

Motivated by the above observations, this paper proposes a distributed control protocol comprising topology control and kinetic control. A localized topology-control rule called β-angle test (BAT) is employed to solve the proposed topology-control problem. Afterwards, the leader-follower flocking problem observed in a three-dimensional UAV swarm scenario is considered, in which the distance maintaining, velocity matching and collision avoidance problems are analyzed. Finally, the convergence of the proposed control protocol is evaluated, with the upper bound of the node degree analyzed.

The main contributions of this paper are listed as follows:

(1) A modified distributed topology-control rule called β-angle test is proposed, based on which the neighbor selection can be performed in the UAV swarm.

(2) A distributed kinetic control protocol is designed to achieve flocking of the UAV swarm under a leader-follower scheme by utilizing the local neighbors' information.

(3) The existence of boundedness of the node-degree of the proposed BAT rule is proved, guaranteeing that the resulting network has a constant maximum node degree. Furthermore, the optimal β value for optimizing the UAV swarm's convergence is also calculated.

The remainder of this paper is organized as follows. Section 2 first introduces the background knowledge of graph theory. After which the kinetic model and leader-follower mechanism are described, followed by defining the convergence metrics. The definition and pseudocode of the proposed BAT algorithm are provided in Section 3, succeeded by introducing kinetic control function. In Section 4, the proposed control function's convergence is analyzed by proving the proposed function's velocity consensus and collision avoidance. In Section 5, the boundedness of node degree of the BAT graph is proved, with the optimal value of parameter β in terms of convergence analyzed. Furthermore, numerous simulation results are presented in Section 6. Unltimately, the conclusion is drawn in Section 7.

2 Preliminaries

2.1 Graph theory

Considering a typical FANET comprising N UAVs, we assume that all the UAVs are identical in terms of physical size and communication/control capabilities. The communication radius of each UAV is assumed to be R. Meanwhile, half-duplex (HD) mode is assumed in the communication link between each pair of neighboring UAVs. The topology of the FANET can thus be modelled as an undirected graph $(\mathcal{V}, \mathcal{E})$, where $\mathcal{V} = \{1, 2, \ldots, N\}$ denotes the set of vertices that correspond to the swarm of UAVs, while $\mathcal{E} = \{(i, j)|i, j \in \mathcal{V}, i \neq j\}$ represents the set of edges between vertices that denote the inter-UAV links. The adjacency matrix $\mathcal{A} = [a_{ij}] \in \mathbb{R}^{N\times N}$ of the undirected graph $(\mathcal{V}, \mathcal{E})$ can be defined by [24]

$$a_{ij} = \begin{cases} 1, & (i, j) \in \mathcal{E}, \\ 0, & \text{otherwise.} \end{cases} \tag{1}$$

The Laplacian matrix $L = [l_{ij}] \in \mathbb{R}^{N\times N}$ is

$$l_{ij} = \begin{cases} \sum\limits_{k=1,k\neq i}^{N} a_{ik}, & i = j, \\ -a_{ij}, & i \neq j. \end{cases} \tag{2}$$

Note that L is symmetric, because $\mathcal{E}$ is an undirected graph.

2.2 UAV kinetic model

In the UAV swarm comprising N agents, the kinematic equation of each UAV in the three-dimensional space can be described as follows [25]:

$$\begin{cases} \dot{p}_i = v_i, \\ \dot{v}_i = u_i, \end{cases} \quad \forall i \in \mathcal{V}, \tag{3}$$

where $p_i \in \mathbb{R}^3$ denotes the position of i-th UAV, while v_i and u_i denote the velocity and control input of i-th UAV, respectively. With some abuse of notation, we use bold font to represent vector variables that are related to the information of a whole swarm, e.g., $\boldsymbol{p}$ and $\boldsymbol{v}$ define the position and velocity vectors of a swarm, respectively. The state variables of an individual node under Euclidean coordinates are distinguished by normal font with subscripts, e.g., p_i and v_i corresponds to the position and velocity of the i-th node, respectively. The neighbor set of the i-th UAV is denoted by $\mathcal{N}_i$:

$$\mathcal{N}_i = \{ j \in \mathcal{V} \,|\, \|ij\| \leqslant r \}, \tag{4}$$

where $\|ij\| = \|p_i - p_j\|$ represents the relative distance between the i-th and j-th UAVs. Initially, the swarm of the UAVs are randomly deployed, provided that the connectivity of the network must be guaranteed in the initial deployment. The selected neighbor set of the i-th UAV can thus be determined by using the topology-control algorithm:

$$\mathcal{N}_i^c = \{ j \in \mathcal{N}_i \,|\, (i,j) \in \mathcal{E}_i^c \}, \tag{5}$$

where $\mathcal{E}_i^c$ denotes the edges that satisfy the proposed topology-control condition in the i-th UAV's neighborhood set, as proposed in Subsection 3.1. Obviously, $\mathcal{N}_i^c \subseteq \mathcal{N}_i$ can be satisfied.

2.3 Leader-follower mechanism

Assume that the FANET comprises one leader and $N-1$ followers, each UAV can establish communication links with its connecting neighbors following the proposed BAT rule. Upon receiving the assignment information from the control center, the leader UAV will proceed to the destination following the designed trajectory, while the follower UAVs are unaware of the destination simply because these followers have no contact ties with the control center. Under the above-mentioned policy, the followers can adjust their dynamics in accordance with their neighbors to both achieve a velocity consensus and maintain a constant relative distance between neighbors. Note that the leader UAV is itself located in the neighbor set of its followers. Moreover, it follows the proposed topology-control rule. The leader's control input is given by

$$u_l = f(t), \quad f(t) \in \mathbb{R}^3, \tag{6}$$

where $f(t)$ denotes a bounded control input from the external orders. In the following, the subscript l denotes the state variable of the leader UAV. For example, p_l and v_l represent the corresponding position and velocity of the leader UAV, respectively. The leader UAV together with its followers select their neighbors following the same rule, while their control input function could be different.

2.4 Convergence metrics

In this part, the metrics of convergence is defined for evaluating the effectiveness of the proposed control protocol. Denote the graph generated by the proposed neighbor selection rule in this paper by $(\mathcal{V}, \mathcal{E}^c)$. In terms of the ratio of connected neighbors reaching the ideal relative distance l_0 between a UAV and its neighbors, we present the following definition:

$$\gamma^* = \frac{\sum_{i \in \mathcal{V}} N_i^{c*}}{\sum_{i \in \mathcal{V}} N_i^c}, \tag{7}$$

where N_i^c denotes the number of connected nodes in $\mathcal{N}_i^c$, and N_i^{c*} represents the number of connected node pair $(i,j) \in \mathcal{E}^c$ that satisfies $|\|ij\| - l_0| \leqslant \varepsilon^*$, for some small error ε^*. Obviously, γ^* is in the range $[0,1]$. A higher value implies that more connections have reached their desired distance. Following this rule, the convergence of the proposed protocol can be improved.

To evaluate the convergence in terms of both the relative distance control and the velocity consensus, the standard deviations of the distance and velocity of the leader UAV relative to its followers are given by

$$d^* = \sqrt{\frac{1}{\sum_{i\in\mathcal{V}} N_i^c} \sum_{i\in\mathcal{V}} \sum_{j\in\mathcal{N}_i^c} \hat{p}_{ij}^{\mathrm{T}} \hat{p}_{ij}} \tag{8}$$

and

$$v^* = \sqrt{\frac{1}{N} \sum_{i\in\mathcal{V}} \hat{v}_i^{\mathrm{T}} \hat{v}_i}, \tag{9}$$

respectively, where $\hat{p}_{ij} = \|ij\| - l_0$ and $\hat{v}_i = v_i - v_l$ denote the distance and velocity vectors relative to the desired value, respectively. Obviously, the lower d^* and v^* values correspond to a superior convergence.

3 Topology control and kinetic control algorithms design

3.1 BAT topology control algorithm

In this part, a distributed topology-control algorithm called β-angle test is proposed for removing the unnecessary communication links from the object UAV's neighborhood set. As the number of neighbors located inside a UAV's communication range increases, minimizing redundant connections can avoid unnecessary computation and communication overhead. Thus, the proposed topology-control protocol should have a bounded node degree, i.e., the maximum number of connections to any node in the swarm should be less than a given constant. Furthermore, the proposed protocol should be capable of employing each agent's local information for achieving the distributed characteristic where the local information is restricted to the information of that agent's one-hop neighbors. Meanwhile, the topology graph constructed by the topology-control algorithm should be symmetric to guarantee a bidirectional communication link between agents. In addition, at the initial stage, each agent selects a fraction of neighbors to be its connected neighbors under the proposed topology-control condition. After this, the agent takes those neighbors as references for adjusting its own position and velocity. Moreover, the relative distance between this agent and its connected neighbors is maintained. Based on the AAT algorithm, an improved topology-control rule called β-angle test is defined as follows.

Definition 1. For a graph G whose vertices are $\mathcal{V}$, the edge between the i-th and the j-th nodes $(i,j \in \mathcal{V})$ can be established if and only if the inner angle $\angle ikj$ satisfies $\angle ikj < \beta$ for any node $k \in \mathcal{V}\backslash\{i,j\}$, where $\beta \in (0,\pi)$.

The graph determined by both β and ij, denoted by $BG(ij,\beta)$, is the union set of two disks, in which ij stands for the chords of both disks. The corresponding angle of circumference is denoted by β. Furthermore, the radii of both disks can be calculated as $R_{BG} = \frac{\|ij\|}{2\sin\beta}$.

For the i-th UAV, it evaluates both the relative distance and direction of neighbor agents relying on techniques such as time of signal arrival (TOA) and angle of arrival (AOA) [26, 27]. After that, it will decide whether the connections with its neighbors can be established using BAT rule. Figure 1, from inside to outside, shows three cases corresponding to scenarios where $\beta = 2\pi/3, \pi/2$, and $\pi/3$, respectively. When $\beta = \pi/2$ holds, the BAT rule will be identical to that of AAT, whose curve is a regular circle. The curves represent trajectories of node k satisfying $\angle ikj = \beta$. For a given β, the curve comprises two arcs, which are symmetric about line ij in terms of both the corresponding chord ij and the circumferential angle β. If there exists no other node inside the circle, the i-th and j-th nodes will be BAT connected at β. As shown in Figure 2(a), the i-th and j-th nodes are BAT connected. Observe that β_1, β_2 and β_3 are less than β. However, from Figure 2(b), the i-th and j-th nodes are not BAT

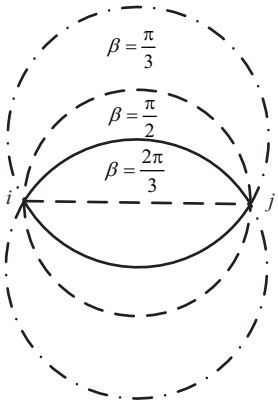

Figure 1 The BAT circles at $\beta = \frac{\pi}{3}, \frac{\pi}{2}$ and $\frac{2\pi}{3}$.

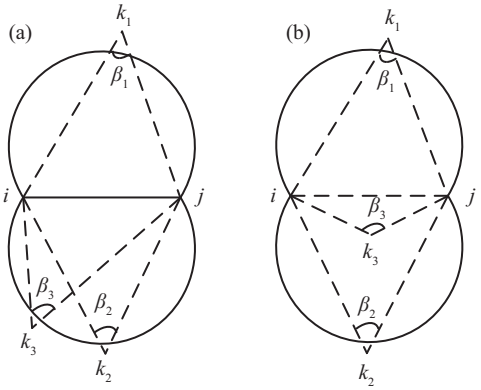

Figure 2 (a) shows that the i-th and j-th nodes are BAT connected. (b) shows that the i-th and j-th nodes are not BAT connected.

connected because $\beta_3 > \beta$. Note that the above description is carried out on a planar plane. Even in three dimensional spaces, it is still applicable to the BAT rule except that the circle is replaced by sphere. Furthermore, the pseudocode of BAT algorithm for the following UAVs is given as Algorithm 1.

Algorithm 1 β-angle test

Require: neighbor position matrix $\boldsymbol{p}_i$ for each UAV i, critical value of β;

```
for j ∈ N_i do
    for k ∈ N_i\{j} do
        calculate ∠ikj;
        if ∠ikj > β then
            a_ij = 0;
            break
        end if
        a_ij = 1;
    end for
end for
return A_i.
```

Compared with topology-control mechanisms such as N-nearest neighbor rule or AAT rule, the proposed BAT rule exhibits several advantages as the following.

(1) In essence, BAT rule follows the concepts of distribution and symmetricity, making the topology structure scalable and robust for FANET as the number of swarm agents increases. Furthermore, by considering the link between two UAV individuals as bidirectional, the BAT rule would be more applicable because the communication between agents generally comprises the request and acknowledgment frames. Thus, the rule must be symmetric to avoid extra problems such as a hidden terminal.

(2) As one of the special cases of BAT, the AAT algorithm merely considers the condition that the angle test threshold is $\beta = \pi/2$. However, the analysis in Section 6 shows that the optimal angle in terms of both system's convergence time and convergence error is not necessarily equal to $\pi/2$, enabling us to select a proper β value that leads to the optimal convergence result.

(3) As the number of nodes in communication range increases, algorithms with full connectivity will cause a huge number of connections for each node, in which the computational complexity will drastically increase. Besides, for the AAT rule, the maximum node degree can reach as much as $n-1$, which is inapplicable in a real FANET with limited channel resources [13]. However, in the BAT rule, it is proved that the maximum node degree is partially bounded in Section 5, making the algorithm be more practical than the original AAT rule.

3.2 Kinetic control function

To avoid collision, maintain relative distance and match velocities between the i-th UAV and their connected neighbors. The control input for the object UAVs must comprise two parts, i.e., the distance control term u_i^p and velocity matching control term u_i^v. The control input is thus given by $u_i = u_i^p + u_i^v$. Specifically, a simplified control function is given by

$$u_i = k_p \sum_{j \in \mathcal{N}_i^c} \left(1 - \frac{l_0}{\|ij\|}\right) p_{ij} - k_v \sum_{j \in \mathcal{N}_i^c} v_{ij}, \tag{10}$$

where both k_p and k_v are constants, whereas $p_{ij} = p_j - p_i$ and $v_{ij} = v_j - v_i$, respectively. Then Eq. (10) can be rewritten in the vector form:

$$\boldsymbol{u} = k_p \left((l_0 \tilde{L} - L) \otimes I_3\right) \boldsymbol{p} + k_v (L \otimes I_3) \boldsymbol{v}, \tag{11}$$

where $\boldsymbol{u} = [u_1^{\mathrm{T}}, \ldots, u_N^{\mathrm{T}}]^{\mathrm{T}}$, $\boldsymbol{p} = [p_1^{\mathrm{T}}, \ldots, p_N^{\mathrm{T}}]^{\mathrm{T}}$, $\otimes$ is the Kronecker product, I_3 denotes a 3×3 identity matrix, and $\tilde{L}$ is the Laplacian matrix corresponding to $\tilde{A} := [\frac{a_{ij}}{\|ij\|}]$ if $(i, j) \in \mathcal{E}^c$. The following goals for the UAV swarm can be reached by using both the proposed neighbor-set-selection rule and the control input function.

(1) Without knowing the leader's information globally, all the following agents in the swarm are capable of moving at the same speed as the leader, i.e., $\lim_{t \to \infty} (v_i(t) - v_l(t)) = 0, \forall i \in \mathcal{V} \backslash \{l\}$ holds, where v_l denotes the leader's velocity.

(2) All the agents are required to keep a fixed relative distance to their connected neighbors, i.e., $\lim_{t \to \infty} \|ij\| = l_0, \forall i \in \mathcal{V}$ and $\forall j \in \mathcal{N}_i^c$, must be satisfied.

(3) The collision of any two UAVs should be avoided. We first simplify the UAV model to be a sphere of radius r_0, following which the minimum distance $d_{\min}$ must satisfy $d_{\min} \geqslant 2r_0$.

4 Stability analysis

In this section, the convergence analysis of flocking in the UAV swarm [28] under the control input in (10) will be presented. Let us first present the following theorem.

Theorem 1. In a swarm comprising N UAVs, including one leader and $N - 1$ followers, the kinetic control of the followers obeys the rule specified in (3). For followers, the control input is acquired from the information of its neighbors under the requirement in (10). After that, all the agents will converge to the same speed with the same distance to their BAT connected neighbors.

Proof. At time $t = t_k, k = 1, 2, \ldots$, the topology of the UAV swarm is assumed to be time-variant. Consider the time slot $[t_k, t_{k+1})$ during which the network topology is fixed, the potential function V_{ij} between the i-th and j-th UAVs is given by

$$V_{ij} = k_p (\|ij\| - l_0)^2. \tag{12}$$

The Lyapunov energy function of the UAV swarm can thus be expressed as

$$E = \sum_{i \in \mathcal{V}} \left(V_i + \frac{1}{2} \hat{v}_i^{\mathrm{T}} \hat{v}_i\right) = \frac{1}{2} \sum_{i \in \mathcal{V}} \left(\sum_{j \in \mathcal{N}_i^c} V_{ij} + \hat{v}_i^{\mathrm{T}} \hat{v}_i\right), \tag{13}$$

where $V_i = \sum_{i \in \mathcal{V}} V_{ij}$ represents the potential function at i-th node. Furthermore, supposing that the initial energy is $E(t_0)$, we can readily conclude that $E(t_0)$ is bounded. By taking the first-order derivative

to the energy function with respect to time, we get

$$\begin{aligned}\dot{E} =&\frac{1}{2}\sum_{i\in\mathcal{V}}\left(\sum_{j\in N_i^c}\dot{V}_{ij}+\hat{v}_i^{\mathrm{T}}\dot{\hat{v}}_i\right)\\ =&\sum_{i\in\mathcal{V}}\left(\sum_{j\in\mathcal{N}_i^c}\dot{p}_i^{\mathrm{T}}\nabla_{p_i}V_{ij}+\hat{v}_i^{\mathrm{T}}\dot{\hat{v}}_i\right)\\ =&\sum_{i\in\mathcal{V}}\hat{v}_i^{\mathrm{T}}\left[\sum_{j\in\mathcal{N}_i^c}k_p\left(\|ij\|-l_0\right)\left(-\frac{p_{ij}}{\|ij\|}\right)+k_p\left(1-\frac{l_0}{\|ij\|}\right)p_{ij}+k_v\sum_{j\in\mathcal{N}_i^c}v_{ij}\right]\\ =&k_v\sum_{i\in\mathcal{V}}\sum_{j\in\mathcal{N}_i^c}\hat{v}_i^{\mathrm{T}}v_{ij}.\end{aligned}\tag{14}$$

Evidently, we have $\dot{E}\leqslant 0$ when $k_v<0$. For each time slot $[t_k,t_{k+1})$, the length of connected edge lies in $(0,R)$, guaranteeing that both the connectivity of the graph $(\mathcal{V},\mathcal{E}^c)$ and collision avoidance can be met. Note that $E(t_0)$ is bounded, i.e., $E(t)\leqslant E(t_k),\forall t\in[t_k,t_{k+1})$ holds.

At $t=t_k$, when the topology of UAV swarm changes, the velocities of all agents remain the same, while the adjacency matrix $\mathcal{A}$ changes owing to the topological changes, e.g., some new connections are established while part of those existing are removed. Obviously, for each edge entry in $\mathcal{E}^c$, we can conclude that V_{ij} is bounded, implying that the energy variation ΔE is bounded. Consequently, it is shown that $E_{t_k^+}=E_{t_k^-}+\Delta E$ is also bounded. Furthermore, we may let the (invariant) level set of E be

$$\Omega=\left\{\hat{p}\in\mathbb{R}^{3N},\hat{v}\in\mathbb{R}^{3N}\,|E\left(\hat{p},\hat{v}\right)\leqslant E_{\max}\right\},\tag{15}$$

where $\hat{p}=[\ldots,p_{ij}^{\mathrm{T}},\ldots]^{\mathrm{T}}$ and $\hat{v}=[\ldots,\hat{v}_i^{\mathrm{T}},\ldots]^{\mathrm{T}}$. Because the connectivity of the network graph $(\mathcal{V},\mathcal{E}^c)$ holds as $t\geqslant t_0$, we can conclude that $\|ij\|$ is bounded. Furthermore, $E\leqslant E_{\max}$ leads to $\|\hat{v}_i\|\leqslant\sqrt{2E_{\max}}$, showing that Ω is compact. Using the non-smooth version of LaSalle's theorem [29], it is shown that the UAV swarm converges to the largest invariant subset $S=\{(\hat{p},\hat{v})|\dot{E}=0\}$. Thus, for all UAVs in the swarm of interest, $\lim_{t\to\infty}\hat{v}_i=0$ and $\lim_{t\to\infty}d_{ij}=l_0,\forall j\in\mathcal{N}_i^c$ can always be guaranteed.

5 Analysis of β in BAT

5.1 Maximum node degree in BAT

Without loss of generality, we denote the graph constructed by node set $\mathcal{V}$ following BAT condition in Definition 1 by $BG(\mathcal{V})$. Furthermore, we denote the graph satisfying the AAT condition by $AG(\mathcal{V})$. Following the above-mentioned definitions, we present the following lemma.

Lemma 1. For the node set $\mathcal{V}\in\mathbb{R}^2$, $BG(\mathcal{V})\supset AG(\mathcal{V})$ is met, if $\forall\beta>\pi/2$, or $BG(\mathcal{V})\equiv AG(\mathcal{V})$ is met, if $\beta=\pi/2$, or $BG(\mathcal{V})\subset AG(\mathcal{V})$ is satisfied, if $\forall\beta<\pi/2$.

Proof. For an arbitrarily chosen node pair (e.g., the i-th and j-th nodes, let us consider the edge ij, where $i,j\in\mathcal{V}$).

In the case that $\beta>\pi/2$, if there exists a node k satisfying $\frac{\pi}{2}<\angle ikj<\beta$, then edge ij satisfies the BAT condition but fails to satisfy the AAT condition. In other words, $ij\in BG(\mathcal{V})$ but $ij\notin AG(\mathcal{V})$. When $\angle ikj>\beta$ is met, we have $ij\notin BG(\mathcal{V})$ and $ij\notin AG(\mathcal{V})$. Furthermore, when $\angle ikj<\pi/2$ is satisfied, we have $ij\in BG(\mathcal{V})$ and $ij\in AG(\mathcal{V})$. In summary, for an arbitrarily chosen edge ij, if $ij\in AG(\mathcal{V})$ is satisfied, then $ij\in BG(\mathcal{V})$ holds as well. Therefore, we get $BG(\mathcal{V})\supset AG(\mathcal{V})$. Similarly, $BG(\mathcal{V})\subset AG(\mathcal{V})$ can be proved by using $\beta<\pi/2$. Obviously, when $\beta=\pi/2$ is satisfied, the AAT condition is shown to be identical to the BAT condition, and we get $BG(\mathcal{V})\equiv AG(\mathcal{V})$. This completes the proof.

In three-dimensional spaces, the above-mentioned statement holds as well. In the following, the node degree boundedness of $BG(\mathcal{V})$ is analyzed. First, let us study the case of two-dimensional space, as given by the following theorem.

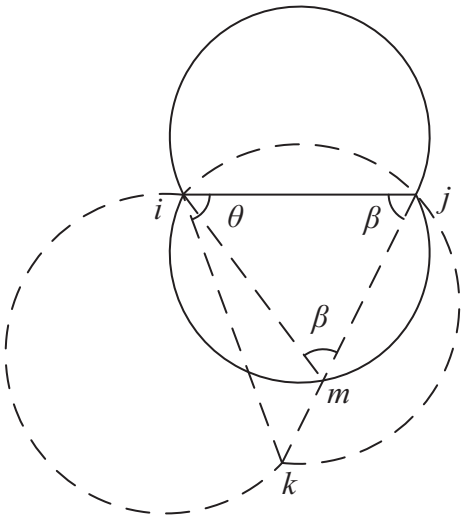

Figure 3 Two adjacent edges ij and ik in $BG(\mathcal{V})$.

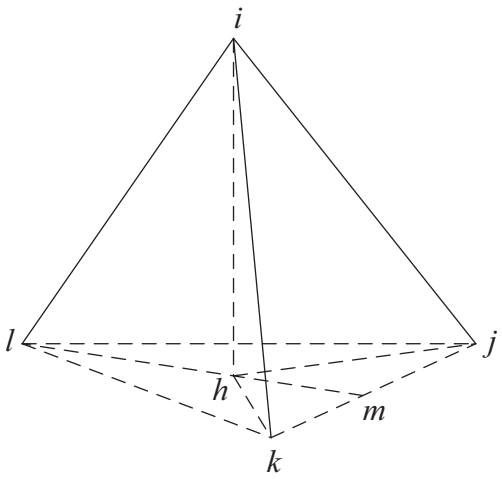

Figure 4 Solid angle of $\triangle jkl$ at i.

Theorem 2. For a set of nodes $\mathcal{V} \in \mathbb{R}^2$, the maximum node degree $d_{\max}(BG(\mathcal{V}))$ of $BG(\mathcal{V})$ under the BAT condition is partially bounded, with the upper bound given by

$$d_{\max}(BG(\mathcal{V})) = \left\lfloor \frac{2\pi}{\pi - 2\beta} \right\rfloor, \quad \forall \beta \in \left(0, \frac{\pi}{2}\right). \tag{16}$$

Proof. For $\beta \geqslant \pi/2$, by following Lemma 1, we get $BG(\mathcal{V}) \supseteq AG(\mathcal{V})$, showing that $AG(\mathcal{V})$ is unbounded [30]. Consequently, $BG(\mathcal{V})$ is unbounded as well.

For $\beta < \pi/2$, we can draw the above-mentioned conclusion by proving that the minimum angle θ enclosed by the adjacent edges in $BG(\mathcal{V})$ has a lower bound [15]. Without loss of generality, we assume that $ij, ik \in BG(\mathcal{V})$ and $\|ij\| \leqslant \|ik\|$. Specially, when j is on the border of $BG(ik, \beta)$, we get $\angle ijk = \beta$ inside $BG(ik, \beta)$ and $\angle imj = \beta$ inside $BG(ij, \beta)$, as shown in Figure 3. Therefore, we have $\|ij\| = \|im\|$. Because $\|jk\| \geqslant \|ij\|$ is satisfied, k must be on line jm with $\|jk\| \geqslant \|jm\|$. When k is located at m, the corresponding $\angle kij$ (i.e., θ) reaches its minimum, i.e., $\theta_{\min} = \pi - 2\beta$. Therefore, the maximum node degree can be expressed as $d_{\max}(BG(\mathcal{V})) = \lfloor \frac{2\pi}{\pi - 2\beta} \rfloor$. where $\lfloor \cdot \rfloor$ denotes the integer part of the value.

Following the analysis above, we can conclude that $d_{\max}(BG(\mathcal{V}))$ is partially bounded in two-dimensional space under condition $\beta \in \left(0, \frac{\pi}{2}\right)$. Similarly, in three-dimensional space, the following theorem is true.

Theorem 3. For a set of nodes $\mathcal{V} \in \mathbb{R}^3$, the maximum node degree $d_{\max}(BG(\mathcal{V}))$ of $BG(\mathcal{V})$ under the BAT condition is partially upper bounded by

$$d_{\max}(BG(\mathcal{V})) = \left\lfloor \frac{2\pi}{\pi - 3\arcsin \frac{\sqrt{3 - \cot^2 \beta}}{2}} \right\rfloor, \quad \forall \beta \in \left(0, \frac{\pi}{2}\right). \tag{17}$$

Proof. Following Theorem 2, we consider the case where $\beta \in (0, \pi/2)$. Assume that the angle θ enclosed by two adjacent edges in $BG(\mathcal{V})$ reaches its minimum, i.e., $\theta = \pi - 2\beta$. In the following, let us consider the solid angle subtended by the tetrahedron $ijkl$ at vertex i, as shown in Figure 4.

Assume that three adjacent edges $ij, ik, il \in BG(\mathcal{V})$ have a common vertex i with $ih \perp \triangle jkl$. The angle enclosed by adjacent edges in $BG(\mathcal{V})$ is then expressed by $\angle jik = \angle kil = \angle lij = \theta_{\min}$, in which one has $\|ij\| = \|ik\| = \|il\|$ and $\triangle jkl$ as a regular triangle. Evidently, we have $lm \perp jk$. Let the edges be the desired length, as defined in (12), i.e., $\|ij\| = l_0$, we can express $\|ih\|$ as

$$\|ih\| = \sqrt{\|ij\|^2 - \|jh\|^2} = \sqrt{l_0^2 - \left(\frac{2l_0 \cos\beta}{\sqrt{3}}\right)^2} = l_0 \sqrt{1 - \frac{4}{3}\cos^2\beta}. \tag{18}$$

The solid angle of $\triangle hmj$ at vertex i can be given by

$$\begin{aligned}\omega_{\triangle hmj} =& \arcsin\left(\frac{\|mj\|}{\sqrt{\|mj\|^2+\|mh\|^2}}\right) - \arcsin\left(\frac{\|mj\|}{\sqrt{\|mj\|^2+\|mh\|^2}}\frac{\|ih\|}{\sqrt{\|ih\|^2+\|mh\|^2}}\right)\\ =& \arcsin\left(\frac{\|mj\|}{\sqrt{3}\|mj\|}\right) - \arcsin\left(\frac{\|mj\|}{\sqrt{3}}\frac{l_0\sqrt{1-\frac{4}{3}\cos^2\beta}}{\sqrt{l_0^2\left(1-\frac{4}{3}\cos^2\beta\right)+\left(2l_0\cos^2\beta\right)}}\right)\\ =& \frac{\pi}{3} - \arcsin\frac{\sqrt{3-\cot^2\beta}}{2}.\end{aligned} \tag{19}$$

Because $\triangle jkl$ is a regular triangle, we have $\omega_{\triangle hjk} = \omega_{\triangle hkl} = \omega_{\triangle hlj} = 2\omega_{\triangle hmj}$. The solid angle is then given by

$$\Omega_{\triangle jkl} = 6\omega_{\triangle hmj} = 2\pi - 6\arcsin\frac{\sqrt{3-\cot^2\beta}}{2}. \tag{20}$$

Therefore, the maximum node degree is given by

$$d_{\max} = \left\lfloor\frac{4\pi}{\Omega_{\triangle jkl}}\right\rfloor = \left\lfloor\frac{2\pi}{\pi - 3\arcsin\frac{\sqrt{3-\cot^2\beta}}{2}}\right\rfloor. \tag{21}$$

Note that when $\lim_{\beta\to\pi/2} d_{\max} = +\infty$, it indicates that the maximum node degree has no upper bound in AAT algorithm. In order to ensure that the resulting network has a constant maximum node degree, β should be chosen as a value different from $\pi/2$.

5.2 Optimal β in terms of convergence

In this part, the parameter β in the BAT rule is analyzed. As a matter of fact, it is easy to find out the exclusion zone for link ij, as denoted by $BG(ij,\beta)$:

$$\begin{aligned}S_{BG} &= 2\left(\pi\left(\frac{\|ij\|}{2\sin\beta}\right)^2\left(1-\frac{2\beta}{2\pi}\right) + \frac{1}{2}\|ij\|\frac{\|ij\|}{2\tan\beta}\right)\\ &= \frac{\|ij\|^2}{2}\left(\cot\beta + (\pi-\beta)\csc^2\beta\right).\end{aligned} \tag{22}$$

By taking partial derivative to S_{BG} with respect to β, one obtains

$$\frac{\partial S_{BG}}{\partial\beta} = -\|ij\|^2\left(1+(\pi-\beta)\cot\beta\right)\csc^2\beta \leqslant 0. \tag{23}$$

Obviously, β is distributed inside the range $(0,\pi)$, and $\frac{\partial S_{BG}}{\partial\beta} = 0$ is met if and only if $\beta = 0$ is satisfied. In other words, S_{BG} is a monotonically decreasing function of β. Thus the exclusion zone shrinks as β increases, implying that more links can be established at each node. On the one hand, this may lead to an increasing number of neighbors satisfying BAT rule, making it harder to achieve the consensus of relative distance, as shown in Figure 5(a) and (b). The increased number of edges in the resulting network, however, results in a graph with greater algebraic connectivity [31], leading to a higher rate of convergence to global consensus. At the same time, the reference information of velocity from neighboring nodes is enhanced, making it easier for nodes to reach a globally consistent velocity, as shown in Figure 5(c). Moreover, the overall effect mentioned in the above can be seen in curves plotted in Figure 5(d).

The corresponding parameter β is originally set to be $\pi/2$ in the AAT rule. However, simulation results show that $\beta = \pi/2$ is not the optimal value in terms of convergence, in which we have assumed that the velocity of the leader is a constant value and β can be chosen in the range of $[0.9, 1.8]$ in radians with an interval of 0.05. For each β, the simulation is repeated 100 times, followed by adopting the mean value of the metrics. Furthermore, three curves are plotted in each graph, each one representing a unique

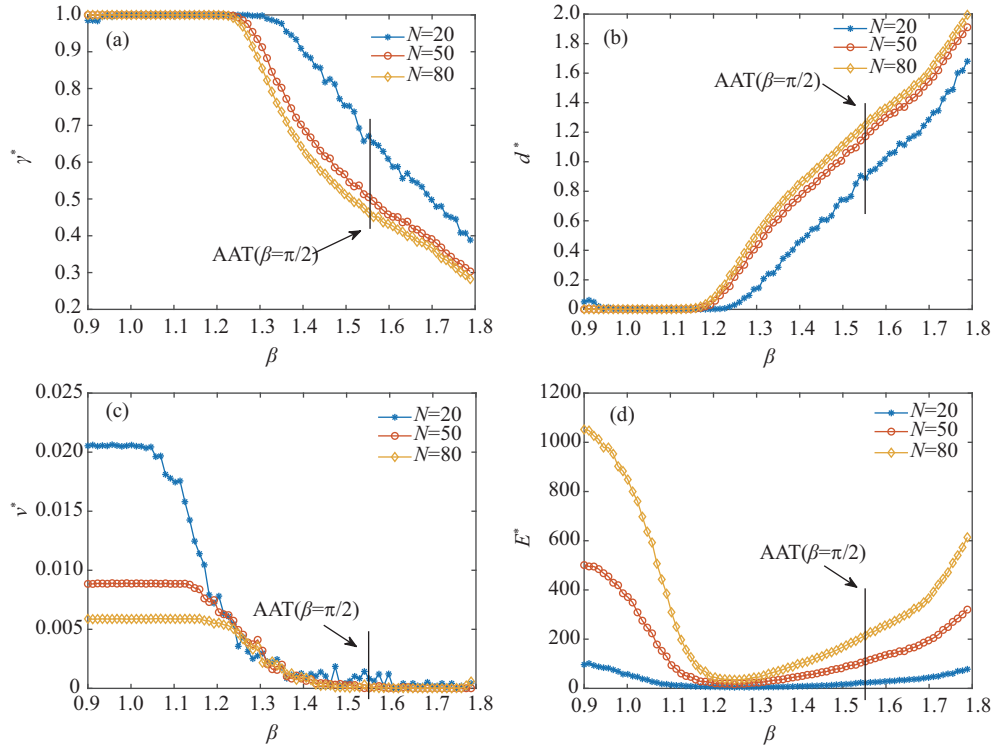

Figure 5 (Color online) γ^* (a), d^* (b), v^* (c) and E^* (d) under different β at $N = 20, 50,$ and 80.

size of swarm (i.e., containing 20, 50, and 80 nodes, respectively). Thereby, the correlation between γ^* in (7) and β is analyzed, together with the impacts of the distance standard deviation d^* in (8), velocity standard deviation v^* and final energy E in (13) considered.

It is worth mentioning that following the BAT rule, the parameter β determines the area in which the neighboring nodes are prohibited from being present. In Figure 5(a), it shows the curves between γ^* and β. As β increases, it is shown that γ^* decreases to its minimum value if $\beta > 1.2$, implying that smaller β value enhances the ratio of connections reaching the preset value l_0. However, when $\beta < 1.2$, the nearly optimal result can be attained.

Note that the same case goes for d^*: when $\beta < 1.2$, the distance standard deviation reaches its nearly optimal value. As β goes larger, the convergence of distance, according to Figure 5(b) gets worse. However, as shown in Figure 5(c), the velocity difference becomes smaller v^* as β increases, thereby reaching its minimum at $\beta \approx 1.2488$. In conclusion, a larger β results in a better convergence in terms of velocity. Therefore, there is a trade-off between achieving optimal velocity consensus and optimal relative distance consensus.

Following the discussion above, neither choosing a larger nor smaller β is appropriate for reaching the optimal convergent. We can thus use the virtual energy to measure the convergence of both velocity and relative distance. As shown in Figure 5(d), the curves become nearly V-shaped and the virtual energy of the swarm reaches its minimum at $\beta \approx 1.2488$. Compared with the corresponding value at $\beta = \pi/2$ (i.e., the AAT rule, as shown in the circled part of the graphs), the γ^* curve shows a better convergence under all the above-mentioned metrics. As a result, the optimal β value is located at $\beta \approx 1.2488$ rather than at $\beta = \pi/2$.

6 Simulation results

In this part, numerical results for both the control protocol in (10) and the proposed BAT rule are presented. The communication radius of the UAVs is assumed to be identical (we set it to be $R = 30$) and the number of UAVs is $N = 50$. In particular, for the kinetic control function, the desired relative

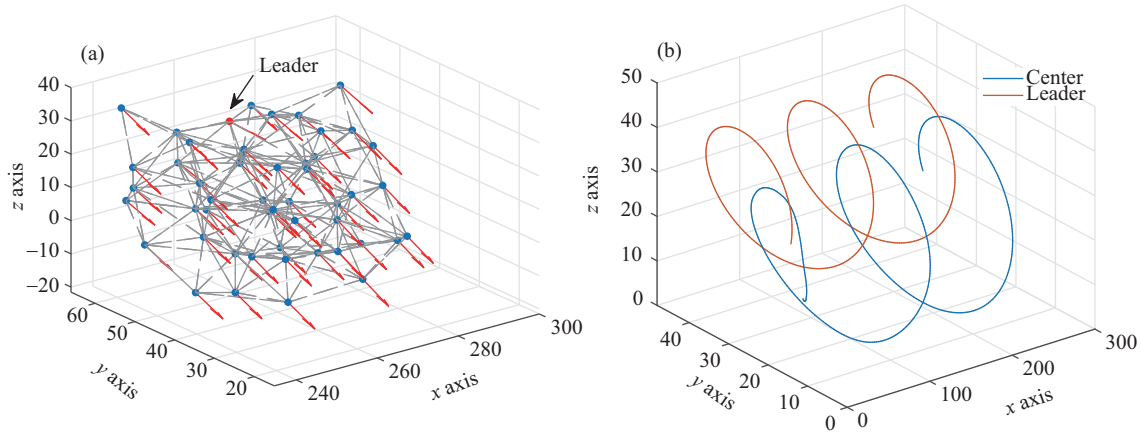

Figure 6 (Color online) Final state and trajectories of UAVs. (a) Final state of all UAVs; (b) trajectories of UAV swarm center and leader.

distance between connected neighbors is set to be $l_0 = 15$. Furthermore, coefficients in (10) are set to be $k_p = 0.17$ and $k_v = -0.1$, respectively [32]. Moreover, as for the topology control, β is set to be 1.2. Initially, the motion states of UAVs including position and velocity are randomly distributed vectors in the range $[0, 1]$ in a three-dimensional space. The initial positions of UAVs are randomly distributed with the connectivity of the network being guaranteed. In addition, 500 iterations are run in each simulation.

The trajectory of the leader UAV is a helix curve expressed by

$$\begin{cases} \hat{p}_l = v_l, \\ v_l = v_x \left[1, \sin(t), \cos(t)\right]^{\mathrm{T}}. \end{cases} \tag{24}$$

The initial position p_l is randomly generated in each simulation together with the follower UAVs and $v_x = 1$. In Figure 6(a), the final state of a UAV swarm is illustrated by arrows to indicate the velocity of the UAVs. The curves between nodes represent the connected neighbors using the proposed BAT rule. As shown in Figure 6(a), the velocities of all nodes converge identically in both direction and magnitude. The UAV swarm's center and leader trajectories (instead of all node trajectories) are given by Figure 6(b) for clarity. Therefore, the desired leader-follower movement can be attained. The clusters center denotes the mean position of all nodes given by $p_c = \frac{1}{N}\sum_{i=1}^{N} p_i$.

To further demonstrate the effectiveness of the control input (10) and the proposed BAT, three cases with variant β values are simulated using a scenario in which the leader's velocity is kept constant. The chosen β values are 1.2, $\pi/2$ and 1.7, representing the cases where β is acute, right (i.e, the AAT rule) and obtuse, respectively. Furthermore, the virtual energy curves during the iterations are given in Figure 7(d). It is shown that the energy E reaches its minimum at about 70 iteration steps, denoting the final energy level that the UAV swarm can be reached.

Because the leader's velocity changes dynamically, it is unrealistic that all the distances between connected neighbors reach l_0 accurately. Thereby, γ^* is used to evaluate the convergence of the relative distance. As shown in Figure 7(a), at $\beta = 1.2, \pi/2$ and 1.7, the corresponding ratios of reaching l_0 within the desired error $\varepsilon^* = 0.05 l_0$ are 0.4, 0.4, and 1, respectively. It is shown that γ^* almost reaches 1 at $\beta = 1.2$, compared with the corresponding value $\gamma^* = 0.4$ under the AAT rule (i.e., $\beta = \pi/2$). Furthermore, Figures 7(b) and (c) denote the standard deviation curves of relative distance and velocity between the followers and the leader during each iteration, as defined in (8) and (9), respectively. At $\beta = 1.2$, the relative distance reaches 0, less than the corresponding values at both $\beta = 1.2$ and $\beta = \pi/2$.

7 Conclusion

In this paper, the flocking of a swarm of UAVs was studied in a leader-follower mode under a distributed kinetic control protocol and topology control rule. In each swarm, a UAV can decide its motion by

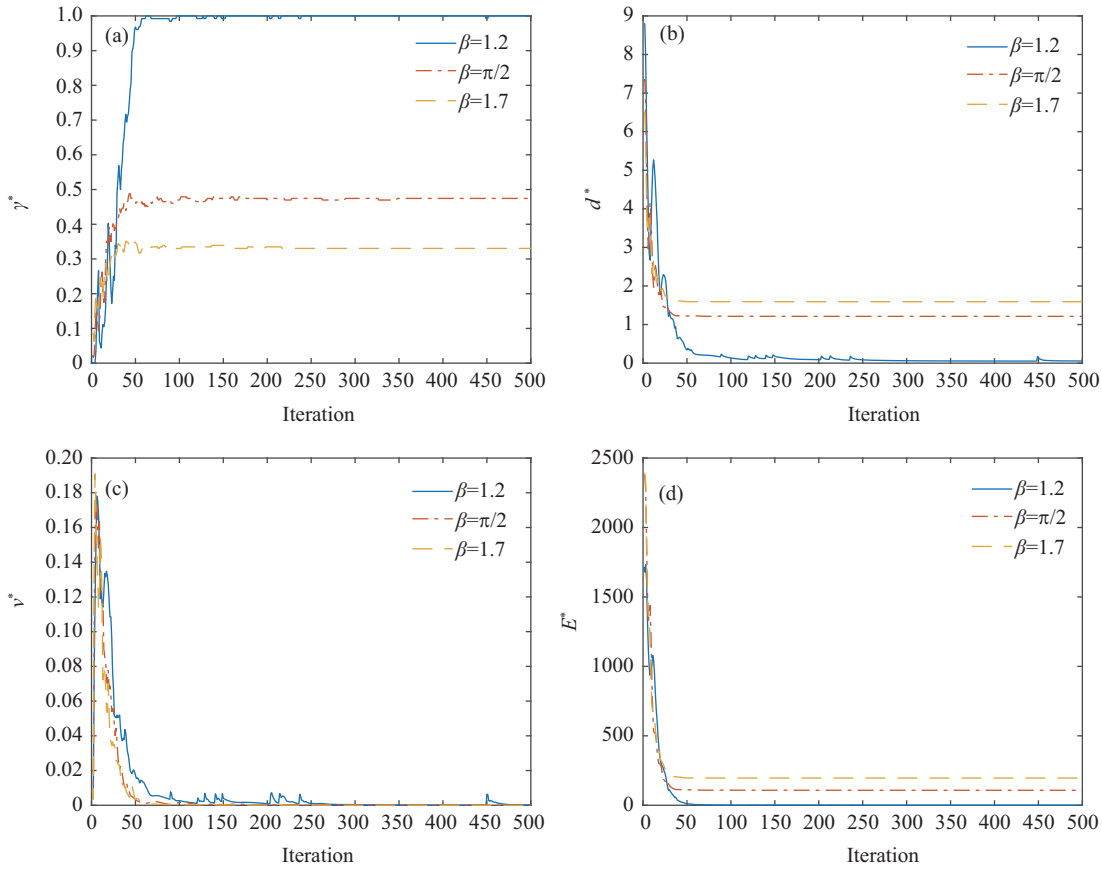

Figure 7 (Color online) γ^* (a), d^* (b), v^* (c) and E^* (d) at each iteration.

following the designed second-order integrator-control-input, in which condition the reference neighbors are chosen by using the BAT-based topology control algorithm. Note that the BAT-based topology control algorithm extends the AAT rule. In addition, each UAV can be designed to select its neighbors that satisfy the condition of its exclusion zone determined by the parameter β. Furthermore, the stability of the proposed control function and the node degree boundedness were analyzed. Moreover, to achieve a better convergence status than the original AAT rule, the optimal β value was analyzed. Simulations were finally carried out to verify the proposed theoretical model. More practical limitations, such as interference, delay and other communication constraints, should also be taken into account in the future to make the proposed model more feasible in a FANET.

Acknowledgements This work was supported in part by Foundation of Beijing Engineering and Technology Center for Convergence Networks and Ubiquitous Services, Joint Foundation of the Ministry of Education (MoE) and China Mobile Group (Grant No. MCM20160103), and Beijing Institute of Technology Research Fund Program for Young Scholars.

References

1 Bekmezci I, Sahingoz O K, Temel S. Flying ad-hoc networks (FANETs): a survey. Ad Hoc Netw, 2013, 11: 1254–1270
2 Hassanalian M, Abdelkefi A. Classifications, applications, and design challenges of drones: a review. Prog Aerospace Sci, 2017, 91: 99–131
3 Cardieri P. Modeling interference in wireless ad hoc networks. IEEE Commun Surv Tutor, 2010, 12: 551–572
4 Xu J J, Xu L, Xie L H, et al. Decentralized control for linear systems with multiple input channels. Sci China Inf Sci, 2019, 62: 052202
5 Zhang Z S, Long K P, Wang J P, et al. On swarm intelligence inspired self-organized networking: its bionic mechanisms, designing principles and optimization approaches. IEEE Commun Surv Tutor, 2014, 16: 513–537
6 Vicsek T, Czirók A, Ben-Jacob E, et al. Novel type of phase transition in a system of self-driven particles. Phys Rev Lett, 1995, 75: 1226–1229
7 Duan H B, Yang Q, Deng Y M, et al. Unmanned aerial systems coordinate target allocation based on wolf behaviors. Sci China Inf Sci, 2019, 62: 014201

8 Rong B, Zhang Z, Zhao X, et al. Robust superimposed training designs for MIMO relaying systems under general power constraints. IEEE Access, 2019, 7: 80404–80420
9 Lu Z H, Zhang L, Wang L. Controllability analysis of multi-agent systems with switching topology over finite fields. Sci China Inf Sci, 2019, 62: 012201
10 Hildenbrandt H, Carere C, Hemelrijk C K. Self-organized aerial displays of thousands of starlings: a model. Behaval Ecol, 2010, 21: 1349–1359
11 Reynolds C W. Flocks, herds and schools: a distributed behavioral model. In: Proceedings of the 14th Annual Conference on Computer Graphics and Interactive Techniques, 1987. 25–34
12 Nedić A, Olshevsky A, Rabbat M G. Network topology and communication-computation tradeoffs in decentralized optimization. Proc IEEE, 2018, 106: 953–976
13 Santi P. Topology control in wireless ad hoc and sensor networks. ACM Comput Surv, 2005, 37: 164–194
14 Jia Y N, Li Q, Qiu S Q. Distributed leader-follower flight control for large-scale clusters of small unmanned aerial vehicles. IEEE Access, 2018, 6: 32790–32799
15 Jeng A A, Jan R H. The r-neighborhood graph: an adjustable structure for topology control in wireless ad hoc networks. IEEE Trans Parallel Distrib Syst, 2007, 18: 536–549
16 Young G F, Scardovi L, Cavagna A, et al. Starling flock networks manage uncertainty in consensus at low cost. PLoS Comput Biol, 2013, 9: e1002894
17 Blough D M, Leoncini M, Resta G, et al. The k-neigh protocol for symmetric topology control in ad hoc networks. In: Proceedings of the 4th ACM International Symposium on Mobile Ad Hoc Networking & Computing. New York: ACM, 2003. 141–152
18 Chiwewe T M, Hancke G P. A distributed topology control technique for low interference and energy efficiency in wireless sensor networks. IEEE Trans Ind Inf, 2012, 8: 11–19
19 Tian B M, Yang H X, Li W, et al. Optimal view angle in collective dynamics of self-propelled agents. Phys Rev E, 2009, 79: 052102
20 Shucker B, Bennett J K. Virtual Spring Mesh Algorithms for Control of Distributed Robotic Macrosensors. University of Colorado at Boulder, Technical Report CU-CS-996-05. 2005
21 Ning B D, Han Q L, Zuo Z Y, et al. Collective behaviors of mobile robots beyond the nearest neighbor rules with switching topology. IEEE Trans Cybern, 2018, 48: 1577–1590
22 Li F, Chen Z M, Wang Y. Localized geometric topologies with bounded node degree for three-dimensional wireless sensor networks. EURASIP J Wirel Commun Netw, 2012, 2012: 157
23 Bullo F, Cortes J, Martinez S. Distributed Control of Robotic Networks: a Mathematical Approach to Motion Coordination Algorithms. Princeton: Princeton University Press, 2009, 27
24 Godsil C, Royle G F. Algebraic Graph Theory. Berlin: Springer, 2013
25 Olfati-Saber R. Flocking for multi-agent dynamic systems: algorithms and theory. IEEE Trans Automat Contr, 2006, 51: 401–420
26 Spencer Q H, Jeffs B D, Jensen M A, et al. Modeling the statistical time and angle of arrival characteristics of an indoor multipath channel. IEEE J Sel Areas Commun, 2000, 18: 347–360
27 Rong P, Sichitiu M L. Angle of arrival localization for wireless sensor networks. In: Proceedings of the 3rd Annual IEEE Communications Society on Sensor and Ad Hoc Communications and Networks, Reston, 2006. 1: 374–382
28 Tanner H G, Jadbabaie A, Pappas G J. Flocking in fixed and switching networks. IEEE Trans Automat Contr, 2007, 52: 863–868
29 Shevitz D, Paden B. Lyapunov stability theory of nonsmooth systems. IEEE Trans Automat Contr, 1994, 39: 1910–1914
30 Wang Y, Liu Y J, Guo Z W. Three-dimensional ocean sensor networks: a survey. J Ocean Univ China, 2012, 11: 436–450
31 Fiedler M. Algebraic connectivity of graphs. Czech Math J, 1973, 23: 298–305
32 Derr K, Manic M. Adaptive control parameters for dispersal of multi-agent mobile ad hoc network (MANET) swarms. IEEE Trans Ind Inf, 2013, 9: 1900–1911